Extended time delayed feedback control of stochastic dynamics in a resonant tunneling diode

Niels Majer, Grischa Stegemann, Eckehard Schöll

***Abstract*— The influence of extended time delayed feedback upon the spatio-temporal currentdensity patterns in a double barrier resonant tunnelling diode is investigated in a spatially extended model of this semiconductor nanostructure. The parameters of the device are chosen to reflect a situation where the only stable state of the system is a spatially inhomogeneous "filamentary" steady state. The addition of weak Gaussian white noise to the system gives rise to spatially inhomogeneous self-sustained temporal oscillations that can be quite coherent. It has been shown that applying a single time delayed feedback can either increase or decrease the regularity of the noise-induced dynamics in this spatially extended system. In this work we show that using *multiple* time delayed feedback provides means to increase the temporal regularity even further and enlarges the parameter regime in which no delay-induced bifurcations occur. Using linear stability analysis these effects can be explained in dependence of the delay time, the feedback strength and the memory parameter.**

I. INTRODUCTION

The presence of random fluctuations can seriously affect charge transport in semiconductors [1], which usually leads to deterioration of their performance. However, recently the constructive role of noise in semiconductor devices has been recognized. In particular, noise in semiconductor lasers was shown to induce coherent radiation [2], [3], [4] or to indicate global bifurcations in superlattices [5], whereas in resonant tunneling diodes it can generate quite regular charge transport dynamics, and even lead to spatial homogenization of current density patterns [6].

Generally, noise-induced dynamics depends on the statistics of random fluctuations and their intensity, which are not easily accessible in real practical situation. In [7], [8] a method for manipulation of essential features of noise-induced oscillations was proposed using a delayed feedback scheme that was originally used to control chaos in purely deterministic systems [9]. This technique was demonstrated to be effective for control of noise-induced oscillations in either simple (generic) systems [10], [11] or more complex and even spatially extended systems[12], [13]. In the present work we study the effect of *multiple* time delayed feedback on the stochastic spatio-temporal pattern formation in the DBRT model in comparison with previous results for *single* time delayed feedback in the same system [14]. For parameter values close to, but below, a Hopf bifurcation we show that one can control both the time-scales and the coherence of noise-induced current density patterns and that the use of multiple time delay can significantly increase the temporal regularity even further. Moreover, if the feedback strength is large, the feedback loop can induce bifurcations and leads to complex changes in the deterministic dynamical properties of the system. We show that the use of multiple time delays enlarges the control parameter regime in which the original deterministic properties of the system do not change.

The paper is organized as follows. In Section II the DRBT model is described, and the dynamical properties of the system for our chosen parameters are discussed. Section III is devoted to effects of the extended time delayed feedback upon noise-induced dynamics in the DBRT, and in Section IV we draw conclusions.

II. MODEL OF THE DBRT WITH TIME DELAYED FEEDBACK AND NOISE

In our study we use a deterministic model for the DBRT suggested in [15] with two sources of random fluctuations added as proposed in [6] [1]. Furthermore we use the time delayed feedback scheme which was already applied to this system in [14] and extend it in order to take multiple time intervals into account for the feedback loop:

$$\begin{aligned} \frac{\partial a(x,t)}{\partial t} &= f(a,u) + \frac{\partial}{\partial x}\left(D(a)\frac{\partial a}{\partial x}\right) + D_a\xi(x,t) \\ \frac{\partial u(t)}{\partial t} &= \frac{1}{\varepsilon}\left(U_0 - u - rJ\right) + D_u\eta(t) - KF(t) \\ F(t) &= u(t) - u(t-\tau) + RF(t-\tau) \end{aligned} \tag{1}$$

where all quantities are dimensionless. From the viewpoint of nonlinear dynamics in the deterministic ($D_a = D_u = 0$) and uncontrolled ($K = 0$) case, this is a reaction-diffusion model of activator-inhibitor type, where a is the activator, and u is the inhibitor. The dynamical variable $a(x,t)$ depends on time and space and describes the charge carrier density inside the quantum well in typical units of $10^{10}/\mathrm{cm}^2$, whereas the second variable $u(t)$ depends only on time and is the voltage drop across the device in typical units of $0.35\,\mathrm{mV}$. The net tunneling rate of the electrons through the two energy barriers into and out of the quantum well is modelled by the nonlinear function $f(a,u)$. $D(a)$ is an effective diffusion coefficient and describes the diffusion of the electrons within the quantum well perpendicular to the current flow (along the x-direction). $J = \frac{1}{L}\int_0^L j\,dx$ gives the total current through the device in typical units of $500\,\mathrm{A/cm}^2$, where $j(a,u) = \frac{1}{2}\left(f(a,u) + 2a\right)$ is the local current density within

This work was supported by Deutsche Forschungsgemeinschaft in the framework of Sfb 555.

Institut für Theoretische Physik, Technische Universität Berlin, 10623 Berlin, Germany,schoell@physik.tu-berlin.de

[1] Herewith a misprint in eq. (1) of [6], which gives an erroneous scaling factor ε in the D_u term, is corrected.

the well. The system's width is fixed at a value of $L = 30$ and homogeneous Neumann boundary conditions are used. The first eq. (1) is the local balance equation of the charge in the quantum well, and the second equation represents Kirchhoff's law of the circuit in which the device is operated. The control parameters are the external bias voltage U_0, the dimensionless load resistance r, and ε. The latter, describing the time-scale ratio of the dynamics of u and a, plays the role of a bifurcation parameter which determines the stability of the fixed points in the system [16]. Physically, $\varepsilon = RC/\tau_a$ is related to the load resistance R, and the parallel capacitance C of the attached circuit, normalized by the tunneling time τ_a. The explicit form of the functions $f(a, u)$ and $D(a)$ is given in the appendix and a discussion of the various deterministic bifurcation scenarios can be found in [15], [16]. In eq. (1) we use uncorrelated Gaussian white noise sources ξ and η with noise intensities D_a and D_u in the respective variables:

$$\begin{aligned} \langle \xi(x,t) \rangle = \langle \eta(t) \rangle &= 0 \qquad (x \in [0, L]), \\ \langle \xi(x,t)\xi(x',t') \rangle &= \delta(x-x')\delta(t-t'), \\ \langle \eta(t)\eta(t') \rangle &= \delta(t-t'). \end{aligned} \tag{2}$$

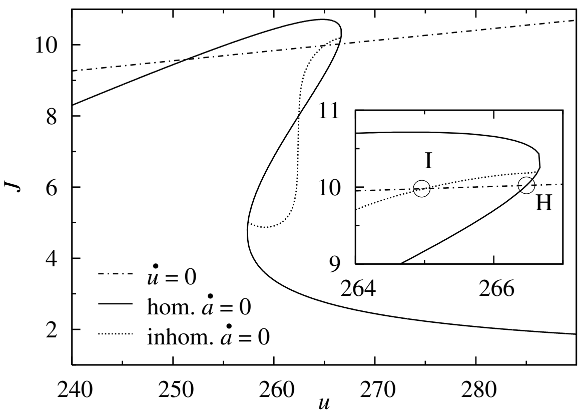

Fig. 1. Current-voltage characteristic of the DBRT model. The null isoclines for the dynamical variables u (which is the load line, dash-dotted) and a in the case of a homogeneous $a(x)$ (solid) and in the case of inhomogeneous $a(x)$ (dotted) are shown. The inset shows an enlargement, where I and H mark the inhomogeneous and the homogeneous fixed points of the system, respectively. $U_0 = -84.2895$, $r = -35$. Other parameters as in [6], [16]. This gives typical units of $500\,\mathrm{A/cm^2}$ for the current density and $0.35\,\mathrm{mV}$ for the voltage.

In the absence of noise and feedback, D_u=$D_a = K = 0$, one can calculate the null isoclines of the system. These are plotted in Fig. 1 using the current-voltage projection of the originally infinite-dimensional phase space. There are three curves, the null isocline $\dot{u} = 0$ (i. e., the *load line*) and two null isoclines $\dot{a} = 0$, one for a reduced system, including only spatially homogeneous states, and one for the full system. We call the system *spatially homogeneous* if the space dependent variable $a(x, t)$ is uniformly distributed over the whole width of the device, i. e. $a(x, t) = a(t)$ for all $x \in [0, L]$, otherwise it is called *spatially inhomogeneous*.

In Fig. 1 one can see the Z-shaped current-voltage characteristic of the DBRT (solid curve), and the inset represents our special region of interest for the following investigations. We fix $\varepsilon = 6.2$ slightly below the Hopf bifurcation, which occurs at $\varepsilon_{\text{Hopf}} \approx 6.469$. In this regime we have a stable, spatially inhomogeneous fixed point marked 'I' in Fig. 1, which is determined by the intersection of the load line (null isocline $\dot{u} = 0$) with the nullcline $\dot{a} = 0$ for inhomogeneous $a(x, t)$. The neighboring intersection of the load line with the homogeneous nullcline (marked 'H') defines another, spatially homogeneous fixed point which is a saddle. It is stable with respect to completely homogeneous perturbations but generally unstable against spatially inhomogenous fluctuations.

It was previously shown that the addition of noise can induce various spatio-temporal patterns in the system [6].

Physically, D_u can be realized by an external tunable noise voltage source in parallel with the supply bias, as used experimentally, e. g., in [3]. In typical dimensional units of $\varepsilon k_{\mathrm{B}}T/e$ [15] $D_u = 1$ corresponds to a parallel noise voltage of $2\,\mathrm{mV}$ at $T = 4\,\mathrm{K}$. D_a describes internal fluctuations of the local current density which could be caused, e. g., by shot noise [1]. The small value of $D_a = 10^{-4}$ used in our simulation gives a noise current density of the order of $50\,\mathrm{mA/cm^2}$, which is within the range of Poissonian shot noise currents $\sqrt{2e\langle I \rangle/\tau_a}$ where $\langle I \rangle$ ist the global mean current.

To measure the temporal ordering of the system, we use the correlation time [17] calculated from the voltage signal u,

$$t_{\text{cor}} \equiv \frac{1}{\sigma^2} \int_0^\infty |\Psi(s)|\, ds, \tag{3}$$

where $\Psi(s) \equiv \big\langle (u(t) - \langle u \rangle)\,(u(t+s) - \langle u \rangle) \big\rangle_t$ is the auto-correlation function of the variable $u(t)$ and $\sigma^2 = \Psi(0)$ its variance.

III. Multiple time delayed feedback control

A. Choice of parameters

The multiple time delayed feedback control introduces, compared to the single time delayed feedback, a new parameter, namely the memory parameter R. Throughout this work the chosen values for R are $R = (0, 0.1, 0.5, 0.9)$, reflecting low, medium and large values of the memory parameter. In the case $R = 0$ the multiple time delayed feedback control scheme reduces to single time delayed feedback control. As shown in [14] the feedback control has its best effect on the regularity of noise induced oscillations for small noise intensities. Therefore we fix the noise intensities at values $D_u = 0.1$ and $D_a = 10^{-4}$.

B. Numerical simulations

In [14] has been shown that the temporal regularity of the noise-induced oscillations in the case of single time delayed feedback depends strongly upon the choice of the delay time τ, where there exist "optimal" τ values for which the correlation time is increased compared to the uncontrolled case and "non-optimal" tau values for which the correlation time is decreased. To see in which way the introduction of a multiple time delayed feedback changes the regularity of the noise induced oscillations compared to the case of single time delay, we keep K fixed at $K = 0.1$ and calculate the correlation time t_c (3) in dependence of τ for the selected values of R. The result is plotted in Fig. 2(a). While for small R the correlation time t_c shows

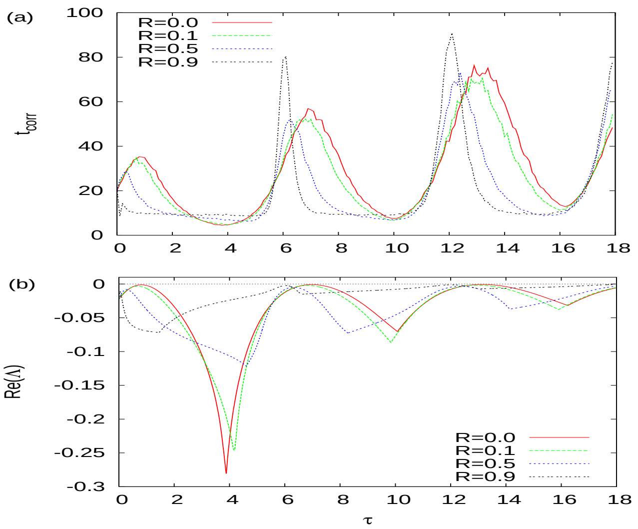

Fig. 2. (a) Correlation time [(3)] for different values of the memory parameter R in dependence of the delay time τ. Red (solid) curves: R=0. Other curves: R≠ 0. (b) Largest realpart Re(Λ) of the linearized deterministic system ($D_u = D_a = 0$) at the inhomogeneous fixed point calculated from Eq. (16).

an oscillatory behaviour, with increasing memory parameter R the peaks in the correlation time become narrower and the region where the correlation time t_c remains at a low value increases. Also, with increasing R the locations of the peaks are shifted to smaller τ values. Comparing the first peak of each curve in Fig. 2(a) we see that for increasing memory parameter R the peak value of tc decreases. For the following peaks though, in the case R=0.9, a measurable increase in correlation time can be observed compared to the case R=0. Fig. 2(b) shows the largest realpart Re(Λ) of the linearized deterministic system ($D_u = D_a = 0$) at the inhomogeneous fixed point calculated from Eq. (16). The location of the maxima of Re(Λ), which determine the stability of the fixed point, correspond to the location of the peaks in correlation time in Fig. 2(a). Therefore, the optimal tau values, for which the correlation time has maxima, is found at tau values where the fixed point is least stable.

C. Analysis of the general form of the characteristic equation

To achieve a deeper understanding of the stability properties of the inhomogeneous fixed point under the influence of the control force we perform a linearization of the original continuous system (1) at the inhomogeneous fixed point along the same lines as in [14].

Introducing

$$a_x \equiv \frac{\partial a}{\partial x}, \qquad a_{xx} \equiv \frac{\partial^2 a}{\partial x^2}, \tag{4}$$

$$b\left(a, a_x, a_{xx}\right) \equiv \frac{\partial}{\partial x}\left(D(a)a_x\right), \tag{5}$$

and a linear operator

$$\mathcal{L} \equiv \left.\frac{\partial f}{\partial a}\right|_{a_0,u_0} + \left.\frac{\partial b}{\partial a}\right|_{a_0} + \left.\frac{\partial b}{\partial a_x}\right|_{a_0}\frac{\partial}{\partial x} + \left.\frac{\partial b}{\partial a_{xx}}\right|_{a_0}\frac{\partial^2}{\partial x^2}, \tag{6}$$

and using the ansatz $\delta a(x,t) = \mathrm{e}^{\Lambda t}\,\tilde{a}(x)$, $\delta u(t) = \mathrm{e}^{\Lambda t}\,\tilde{u}$ for the deviations from the fixed point we can write down the coupled eigenvalue problem:

$$\Lambda\tilde{a}(x) = \mathcal{L}\tilde{a}(x) + f_u(x)\tilde{u}, \tag{7}$$

$$\Lambda\tilde{u} = -\frac{r}{\varepsilon L}\int_0^L j_a(x)\tilde{a}(x)dx + \left[-\frac{1+rJ_u}{\varepsilon} - K\frac{1-\mathrm{e}^{-\Lambda\tau}}{1-R\mathrm{e}^{-\Lambda\tau}}\right]\tilde{u}, \tag{8}$$

$$\text{with } f_u \equiv \left.\frac{\partial f}{\partial u}\right|_{a_0,u_0}, \quad j_a \equiv \left.\frac{\partial j}{\partial a}\right|_{a_0,u_0},$$

$$J_u = \frac{1}{L}\int_0^L \left.\frac{\partial j}{\partial u}\right|_{a_0,u_0} dx.$$

For the case $K = 0$ this eigenvalue problem of the inhomogeneous filamentary fixed point has been analyzed generally [18]. In the voltage-clamped case ($\delta u = 0$), the Sturmian eigenvalue equation $\lambda\tilde{a} = \mathcal{L}\tilde{a}$ with Neumann boundary conditions (which can be shown to be self-adjoint) has solutions $\lambda_0 > \lambda_1 > \lambda_2 > \ldots$ where the corresponding eigenmode $\psi_n(x)$ has n nodes, and $\lambda_0 > 0$, while all other eigenvalues $\lambda_n < 0$ for $n \geq 1$ are stable. The eigenmodes of the full eqs. (7), (8) can be expanded in terms of the voltage-clamped eigenmodes,

$$\tilde{a}(x) = \sum_n \left(\tilde{a}, \psi_n\right)\psi_n(x), \tag{9}$$

where $(\tilde{a}, \psi_n) \equiv \frac{1}{L}\int_0^L \tilde{a}(x)\psi_n(x)dx$ denotes the usual scalar product in Hilbert space. Inserting this into eq. (7) yields

$$\Lambda\sum_n(\tilde{a}, \psi_n)\psi_n(x) = \sum_n \lambda_n(\tilde{a}, \psi_n)\psi_n(x) + f_u(x)\tilde{u}. \tag{10}$$

Forming the scalar product with ψ_m and using orthonormality gives the expansion coefficients

$$(\tilde{a}, \psi_m) = \frac{(f_u, \psi_m)}{\Lambda - \lambda_m}\tilde{u}. \tag{11}$$

The expansion (9) can be inserted into eq. (8):

$$\Lambda\tilde{u} = \left[-\frac{r}{\varepsilon}\sum_n\frac{(f_u, \psi_n)(j_a, \psi_n)}{\Lambda - \lambda_m} - \frac{1+rJ_u}{\varepsilon} - K\frac{1-\mathrm{e}^{-\Lambda\tau}}{1-R\mathrm{e}^{-\Lambda\tau}}\right]\tilde{u}. \tag{12}$$

We will now neglect the higher modes ψ_n because they oscillate fast whereas $a_0(x)$ varies slowly in space, and approximate the sum in eq. (9) by the dominant first term ψ_0 with $\lambda_0 > 0$. We obtain the characteristic equation for the eigenvalue Λ:

$$\Lambda^2 + \left(\frac{1+rJ_u}{\varepsilon} - \lambda_0\right)\Lambda + (\Lambda - \lambda_0)K\frac{1-\mathrm{e}^{-\Lambda\tau}}{1-R\,\mathrm{e}^{-\Lambda\tau}} - \frac{\lambda_0}{\varepsilon}(1+r\sigma_d) = 0, \quad (13)$$

where the static differential conductance at the inhomogeneous fixed point

$$\sigma_d \equiv \left.\frac{dJ}{du}\right|_{a_0,u_0} = J_u + \left(j_a, \frac{da}{du}\right) = J_u - (j_a,\psi_0)\frac{(f_u,\psi_0)}{\lambda_0} \quad (14)$$

has been introduced using eqs. (9), (11) in the static case $\Lambda = 0$ [19]. Without control, $K = 0$, eq. (13) reduces to a characteristic polynomial of second order, which gives the well-known conditions for stability of a filament [18]:

$$A \equiv \frac{1+rJ_u}{\varepsilon} - \lambda_0 > 0, \qquad C \equiv -\frac{\lambda_0}{\varepsilon}(1+r\sigma_d) > 0. \quad (15)$$

Without control a Hopf bifurcation on the two-dimensional center manifold occurs if $A = 0$. With control, eq. (13) can be expressed as

$$\Lambda^2 + A\Lambda + (\Lambda - B)K\frac{1-\mathrm{e}^{-\Lambda\tau}}{1-R\,\mathrm{e}^{-\Lambda\tau}} + C = 0 \quad (16)$$

with $B \equiv \lambda_0 > 0$. The parameters A, B, C can be calculated directly from (15). For the inhomogeneous fixed point $\lambda_0 = 1.0281$ has been calculated in [20]; $J_u = -0.1615$ can be obtained by using the condition for a Hopf bifurcation ($A = 0$) in eq. (15); $\sigma_d = 0.226$ can be estimated from the current-voltage characteristic shown in Fig. 1.

This yields $A = 0.0447$, $B = 1.0281$ and $C = 1.1458$. Note that in dimensional units the unstable eigenvalue of the voltage-clamped system $\lambda_0 = B$ is approximately equal to the inverse tunneling time $1/\tau_a$.

In order to find the boundaries of successful control we separate Eq. (16) into real and imaginary parts and set $Re(\Lambda) = 0$. The boundaries of successfull can then be obtained as a set of parametric functions $K(q)$ and $\tau(q)$ using the imaginary part $q = Im(\Lambda)$ as the curve parameter. The explicit form of this set of parametric equations is quite lengthy and does not provide a deeper insight. Therefore it is omitted. Fig. 3 shows a plot of the domains of successfull control for different values of the memory parameter R calculated from dynamical simulations of the system. The boundaries of successfull control calculated from Eq. (16) are included as red (grey) curves in the figure. It can be seen that they are in good agreement with results obtained from dynamical simulations of the system equations (1). Furthermore, from Eq. (16) it is possible to calculate an

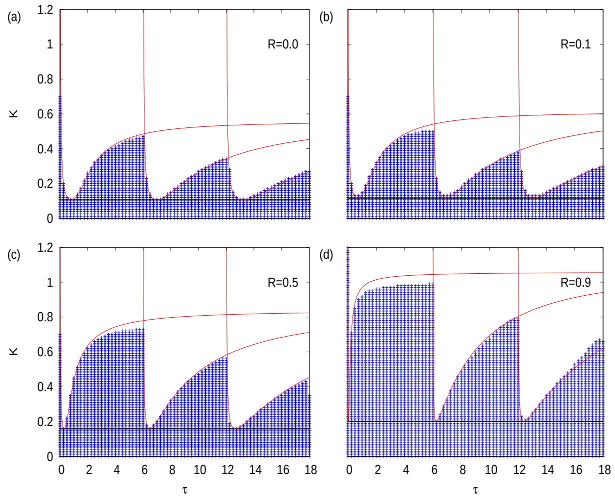

Fig. 3. (a)-(d) Stability region in the τ-K plane of the deterministic system (1) ($D_u = D_a = 0$), for selected values of the memory parameter. The red (grey) curves show solutions to (16) with $Re(\Lambda) = 0$. blue (dark) region: regime of stability of the inhomogeneous fixed point obtained from dynamical simulations.

upper boundary $K_c(R) \sim R$ for the feedback strength, for which no delay-induced bifurcation occurs over the whole τ-interval. These boundaries are included as black lines in Fig. 3. The explicit form again is omitted.

IV. Conclusion

In conclusion we have shown that by introducing a multiple time delayed feedback method the domain of stability of the inhomogeneous fixed point in the τ-K plane enlarges with increasing memory parameter R (Fig. 3) and the parameter regime in K, for which no delay-induced bifurcation occurs increases. Furthermore we have shown that for large enough memory parameter R ($R = 0.9$) and the right choice of the delay time τ it is possible to enhance the regularity of noise induced oscillations compared to single time delayed feedback methods (Fig. 2).

Appendix

*

The effective diffusion coefficient $D(a)$ results from the inhomogeneous lateral redistribution of carriers and from the change in the local potential due to the charge accumulated in the quantum well by Poisson's equation [21]:

$$D(a) = a\left(\frac{d}{r_\mathrm{B}} + \frac{1}{1-\exp(-a)}\right), \quad (17)$$

where d is the effective thickness of the double-barrier structure, $r_\mathrm{B} = (4\pi\epsilon\epsilon_0\hbar^2)/(e^2 m)$ is the effective Bohr radius in the semiconductor material, ϵ and ϵ_0 are the relative and absolute permittivity of the material.

From microscopic consideration of the tunneling currents from the emitter into the quantum well and from there to the emitter one obtain the function f [15]:

$$f(a,u) = \left[\frac{1}{2} + \frac{1}{\pi}\arctan\left(\frac{2}{\gamma}\left(x_0 - \frac{u}{2} + \frac{d}{r_{\mathrm{B}}}a\right)\right)\right]$$
$$\times \left[\ln\left(1 + \exp\left(\eta_e - x_0 + \frac{u}{2} - \frac{d}{r_{\mathrm{B}}}a\right)\right) - a\right] - a. \quad (18)$$

x_0 and γ describe the energy level and the broadening of the electron states in the quantum well and η_e is the dimensionless Fermi level in the emitter, all in units of $k_{\mathrm{B}}T$. Throughout the paper we use values of $\gamma = 6$, $d/r_{\mathrm{B}} = 2$, $\eta_e = 28$ and $x_0 = 114$.

References

[1] Y. M. Blanter and M. Büttiker, "Shot noise in mesoscopic conductors," *Phys. Rep.*, vol. 336, p. 1, 2000.

[2] G. Giacomelli, M. Giudici, S. Balle, and J. R. Tredicce, "Experimental evidence of coherence resonance in an optical system," *Phys. Rev. Lett.*, vol. 84, p. 3298, 2000.

[3] V. V. Sherstnev, A. Krier, A. G. Balanov, N. B. Janson, A. N. Silchenko, and P. V. E. McClintock, "The stochastic laser: mid-infrared lasing induced by noise," *Fluct. Noise Lett.*, vol. 3, p. 91, 2003.

[4] O. V. Ushakov, H. J. Wünsche, F. Henneberger, I. A. Khovanov, L. Schimansky-Geier, and M. A. Zaks, "Coherence resonance near a Hopf bifurcation," *Phys. Rev. Lett.*, vol. 95, p. 123903, 2005.

[5] J. Hizanidis, A. G. Balanov, A. Amann, and E. Schöll, "Noise-induced front motion: signature of a global bifurcation," *Phys. Rev. Lett.*, vol. 96, p. 244104, 2006.

[6] G. Stegemann, A. G. Balanov, and E. Schöll, "Noise-induced pattern formation in a semiconductor nanostructure," *Phys. Rev. E*, vol. 71, p. 016221, 2005.

[7] N. B. Janson, A. G. Balanov, and E. Schöll, "Delayed feedback as a means of control of noise-induced motion," *Phys. Rev. Lett.*, vol. 93, p. 010601, 2004.

[8] A. G. Balanov, N. B. Janson, and E. Schöll, "Control of noise-induced oscillations by delayed feedback," *Physica D*, vol. 199, p. 1, 2004.

[9] K. Pyragas, "Continuous control of chaos by self-controlling feedback," *Phys. Lett. A*, vol. 170, p. 421, 1992.

[10] E. Schöll, A. G. Balanov, N. B. Janson, and A. Neiman, "Controlling stochastic oscillations close to a Hopf bifurcation by time-delayed feedback," *Stoch. Dyn.*, vol. 5, p. 281, 2005.

[11] J. Pomplun, A. G. Balanov, N. B. Janson, and E. Schöll, "Controlling noisy oscillations in nonlinear systems near a Hopf bifurcation," *Phys. Rev. E*, 2007, in preparation.

[12] J. Hizanidis, A. G. Balanov, A. Amann, and E. Schöll, "Noise-induced oscillations and their control in semiconductor superlattices," *Int. J. Bifur. Chaos*, vol. 16, no. 6, pp. 1701–1710, 2006.

[13] A. G. Balanov, V. Beato, N. B. Janson, H. Engel, and E. Schöll, "Delayed feedback control of noise-induced patterns in excitable media," *Phys. Rev. E*, vol. 74, p. 016214, 2006.

[14] G. Stegemann, A. G. Balanov, and E. Schöll, "Delayed feedback control of stochastic spatiotemporal dynamics in a resonant tunneling diode," *Phys. Rev. E*, vol. 73, p. 016203, 2006.

[15] E. Schöll, A. Amann, M. Rudolf, and J. Unkelbach, "Transverse spatio-temporal instabilities in the double barrier resonant tunneling diode," *Physica B*, vol. 314, p. 113, 2002.

[16] J. Unkelbach, A. Amann, W. Just, and E. Schöll, "Time–delay autosynchronization of the spatiotemporal dynamics in resonant tunneling diodes," *Phys. Rev. E*, vol. 68, p. 026204, 2003.

[17] R. L. Stratonovich, *Topics in the Theory of Random Noise*. New York: Gordon and Breach, 1963, vol. 1.

[18] A. Alekseev, S. Bose, P. Rodin, and E. Schöll, "Stability of current filaments in a bistable semiconductor system with global coupling," *Phys. Rev. E*, vol. 57, no. 3, pp. 2640–2649, 1998.

[19] E. Schöll, *Nonlinear spatio-temporal dynamics and chaos in semiconductors*. Cambridge: Cambridge University Press, 2001.

[20] J. Unkelbach, "Rückkopplungsgesteuerte transversale Dynamik der resonanten Tunneldiode," Master's thesis, TU Berlin, 2002.

[21] V. Cheianov, P. Rodin, and E. Schöll, "Transverse coupling in bistable resonant-tunneling structures," *Phys. Rev. B*, vol. 62, p. 9966, 2000.